Acta Cryst. (1980). **B36**, 1007–1014

Structures of $NaTaO_3$ by Neutron Powder Diffraction

BY M. AHTEE

Department of Physics, University of Helsinki, Siltavuorenpenger 20 *D, SF*-00170 *Helsinki* 17, *Finland*

AND C. N. W. DARLINGTON

Department of Physics, The University of Birmingham, PO Box 363, *Birmingham B*15 2*TT, England*

(*Received* 21 *July* 1979; *accepted* 23 *January* 1980)

Abstract

The high-temperature structures of $NaTaO_3$ have been determined by neutron powder profile refinement. At room temperature $NaTaO_3$ is orthorhombic, *Pcmn*, a_o = 5·4842 (2), b_o = 7·7952 (2), c_o = 5·5213 (2) Å, with tilt system $a^-b^+a^-$. With increasing temperature the symmetry changes to *Bmmb* with (at 803 K) a_p = 7·8453 (5), b_p = 7·8541 (8), c_p = 7·8633 (5) Å, and the tilt system to $a^0b^+c^-$. In the tetragonal phase, *C*4/*mmb*, at 893 K, with (conventional tetragonal axes for the corresponding space group *P*4/*mbm*) $a_T = b_T$ = 5·5552 (3), c_T = 3·9338 (4) Å, the second antiphase tilt also disappears producing octahedral tilts described by $a^0b^+a^0$. Comparison is made between these structures, those of $SrZrO_3$ and phase T_1 of $NaNbO_3$, the last of which we have redetermined [space group *Bmmb*, a_p = 7·8592 (3), b_p = 7·8662 (3), c_p = 7·8773 (2) Å]. The structures are also analysed in terms of condensed modes of the high-temperature, cubic phase.

1. Introduction

This paper describes the three non-cubic structures of $NaTaO_3$ found above room temperature and compares them with isostructural phases found in $SrZrO_3$ and $NaNbO_3$. The structural work on $SrZrO_3$ has been published previously (Ahtee, Ahtee, Glazer & Hewat, 1976; Ahtee, Glazer & Hewat, 1978). Here we report a redetermination of the structures of phase T_1 of $NaNbO_3$ (for earlier work see Ahtee, Glazer & Megaw, 1972) and the room-temperature phase of $NaTaO_3$, and for the first time a detailed analysis of the structures of $NaTaO_3$ found in the ranges 753–853 K and 853–903 K.

Ahtee & Unonius (1977) determined the room-temperature structure of $NaTaO_3$ from X-ray powder diffraction patterns by measuring the intensities of the difference reflections caused by deviations from the ideal cubic perovskite structure. They argue that the space group is *Pcmn*, rather than the polar group *Pc*2$_1$*n* suggested by Kay & Miles (1957).

0567-7408/80/051007-08$01.00

Cross (1956) investigated the optical properties of single crystals of $NaTaO_3$ at high temperatures. He found the following sequence of phase transitions:

orthorhombic in rhombic orientation	→	orthorhombic in pseudocubic orientation	→	tetragonal	→	cubic.

Subsequently, Iwasaki & Ikeda (1963), who measured the dielectric constant of $NaTaO_3$, did not find any ferroelectric phase from liquid-helium temperature up to 923 K. They also examined the optical properties of $Na(Nb_{1-x}Ta_x)O_3$ mixed crystals and found, in accordance with Cross, the transition temperatures to be 753, 863 and 913 K for compositions with $x > 0.5$. On the other hand, Ismailzade (1963), who studied $NaTaO_3$ powder by X-ray diffraction methods, concluded that the phase between 753 and 823 K was monoclinic in a pseudocubic orientation, like the room-temperature phase, but with a very small monoclinic angle $\beta - \pi/2 \sim 0.03°$.

2. Experimental

Neutron diffraction measurements were made with the D1A high-resolution powder diffractometer of the high-flux reactor at the ILL (Grenoble). The counter bank, consisting of ten ^{3}He high-pressure counters with 6° angular separation (Hewat & Bailey, 1976), was swept through 2θ = 0 to 160° in steps of 0·05°. The wavelength used was 1·3879 Å. The 20 g, high-purity powder samples (Johnson Matthey Chemicals Ltd, England) were packed in a thin-walled vanadium can. The platinum–rhodium thermocouples used to measure the temperature of the furnace were not calibrated, so that the quoted values for temperature are not absolute values. As the symmetry of $NaTaO_3$ at a measured 873 K is not tetragonal but orthorhombic, it seems that our values for the temperature are about 20 K too high.

In the structure analysis, the profile-refinement technique (Rietveld, 1969; Hewat, 1973) was used. As the number of parameters to be refined was comparatively small – in the room-temperature phase of $NaTaO_3$ 36, in the next orthorhombic phase 40 and in the tetragonal phase only 18 – the final results were obtained by letting all the parameters vary freely. The scattering lengths used were $b_{Ta} = 6{\cdot}91$, $b_{Nb} = 7{\cdot}1$, $b_{Na} = 3{\cdot}62$, $b_O = 5{\cdot}80$ fm (Bacon, 1972).

3. Structure of $NaTaO_3$ at room temperature

In Table 1* the structural parameters of $NaTaO_3$ at room temperature are given according to the space group *Pcmn* suggested by Ahtee & Unonius (1977). When the structure with space group $Pc2_1n$, suggested by Kay & Miles (1957), was refined, Ta had to be fixed at ($\frac{1}{2}$00); the shifts of Na and O(1) along the *y* axis varied between +0·007 (2) and −0·003 (2) in different cycles of the refinement; the shifts of O(2) and O(3) were equal in magnitude. Also, the correlations were very high; between *u*(O2) and *u*(O3): 0·87; *v*(O2), *v*(O3): 0·95; *w*(O2), *w*(O3): 0·90. All these findings favour the space group *Pcmn* rather than $Pc2_1n$. The results of previous authors are compiled in Table 2 for comparison. The structural parameters are given in the orthorhombic orientation using the origin shown in Fig. 1.

In Fig. 1 a diagram of the room-temperature structure of $NaTaO_3$ is given showing one layer of the octahedra in a plane perpendicular to the *b* axis. The orthorhombic unit cell corresponding to the space group *Pcmn* is superposed above the pseudocubic unit cell. This arrangement corresponds to the tilt system $a^-b^+a^-$ of the O atom octahedra, with Na cations within each layer perpendicular to [010] displaced by 0·09 Å parallel to one another, but with displacements in successive layers antiparallel. Using the values of the coordinates specified with respect to the pseudocubic subcell, we find that the octahedra are tilted through 6·9 (4)° about a_p and c_p, and 7·9 (2)° about b_p.

Table 1. *Structural parameters in* $NaTaO_3$ *at room temperature with space group Pcmn*

Isotropic temperature factor refinement

		x	*y*	*z*	*B* (Å²)
Ta	4(*b*)	$\frac{1}{2}$	0	0	0·384 (14)
Na	4(*c*)	−0·0031 (12)	$\frac{1}{4}$	−0·0117 (9)	1·507 (34)
O(1)	4(*c*)	$\frac{1}{2}$−0·0599 (4)	$\frac{1}{4}$	0·0074 (5)	0·842 (29)
O(2)	8(*d*)	$\frac{1}{4}$+0·0357 (3)	−0·0295 (2)	$\frac{1}{4}$+0·0345 (3)	0·897 (18)

$R_{nuclear} = 6{\cdot}56\%$ $R_{profile} = 12{\cdot}41\%$ $R_{expected} = 4{\cdot}86\%$

Anisotropic temperature factor refinement

		B_{eq} (Å²)*
Ta		0·53 (13)
Na	$u = -0{\cdot}0047$ (11), $w = -0{\cdot}0158$ (8)	1·42 (32)
O(1)	$u_1 = -0{\cdot}0619$ (5), $w_1 = 0{\cdot}0092$ (5)	0·82 (18)
O(2)	$u_2 = -0{\cdot}0351$ (3), $v_2 = 0{\cdot}0295$ (2), $w_2 = 0{\cdot}0340$ (3)	0·91 (7)

$a_o = 5{\cdot}4842$ (2) Å $b_o = 7{\cdot}7952$ (2) Å $c_o = 5{\cdot}5213$ (2) Å

$R_{nuclear} = 4{\cdot}63\%$ $R_{profile} = 10{\cdot}64\%$ $R_{expected} = 4{\cdot}85\%$

* $B_{eq} = \frac{1}{3}$ trace $\tilde{\mathbf{B}}$ (Willis & Pryor, 1975).

Table 2. *Comparison of the structural parameters in* $NaTaO_3$ *at room temperature with the results of previous workers*

	This work	Ahtee & Unonius (1977)	Kay & Miles (1957)
Na			
u	−0·0047 (11)	0	0·01
v	0	0	0·03
w	−0·0158 (8)	−0·02 (1)	−0·02
O(1)			
u_1	−0·0619 (5)	−0·054 (1)	−0·02
v_1	0	0	0·01
w_1	0·0092 (5)	0	−0·02
O(2)			
u_2	0·0351 (3)	0·025 (1)	0·04
v_2	−0·0295 (2)	−0·027 (1)	−0·03
w_2	0·0340 (3)	0·025 (1)	0·04
O(3)			
($\frac{1}{4}$+) u_3	0·0351	0·025	0·04
($\frac{1}{2}$+) v_3	0·0295	0·027	0·06
($\frac{1}{4}$+) w_3	0·0340	0·025	0·04

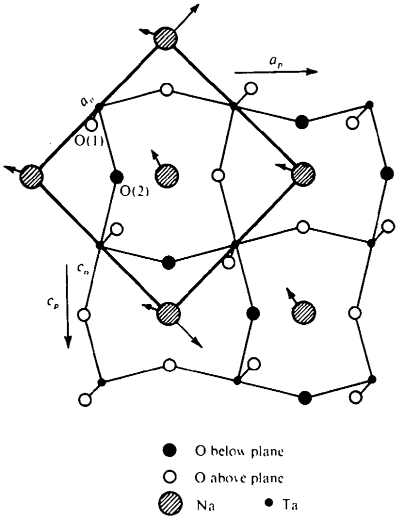

Fig. 1. Diagram of the $NaTaO_3$ structure at room temperature showing both the orthorhombic (thick lines) and pseudocubic unit cells with one layer of octahedra perpendicular to [010].

---

* Lists of anisotropic thermal parameters for $NaTaO_3$ at room temperature, 803 K, 873 K and 893 K, and for $NaNbO_3$ (phase T_1) at 813 K, have been deposited with the British Library Lending Division as Supplementary Publication No. SUP 35040 (3 pp.). Copies may be obtained through The Executive Secretary, International Union of Crystallography, 5 Abbey Square, Chester CH1 2HU, England.

4. Structure of $NaTaO_3$ at 803 and 873 K

In the diffraction patterns of $NaTaO_3$ at both 803 and 873 K there are superlattice reflections, some of which when indexed on the doubled pseudocubic subcell have all odd indices, others having two odd and one even. The former type of reflections indicate antiphase (—) tilts of the octahedra and the latter in-phase (+) tilts. The most likely explanation is, therefore, that the phase is orthorhombic with the tilt system $a^0b^+c^-$ as found in, *e.g.*, $SrZrO_3$ at 1033 K (Ahtee *et al.*, 1978), $CsPbCl_3$ phase III (Fujii, Hoshino, Yamada & Shirane, 1974) and $NaNbO_3$ phase T_1 (Ahtee *et al.*, 1972). The space group of the tilted framework, *Bmmb*, also allows the two independent Na atoms to be displaced along [001] in antiparallel layers perpendicular to [010]. A diagram of the $NaTaO_3$ $a^0b^+c^-$ structure is presented in Fig. 2.

Refinement of this model was carried out and the results are listed in Tables 3 and 4 for the structures at 803 K and 873 K, respectively. The 444 reflection was examined for splitting caused by the monoclinic distortion suggested by Ismailzade (1963). Our results did not reveal any support for the splitting, but the wavelength used was too small to allow a definite conclusion in this respect. Some of the values for the positional parameters depended on whether the refinement included isotropic or anisotropic temperature factors. Because of the large anisotropy of the temperature factors we took the values from the anisotropic refinements to be the more reliable. They are therefore used in all calculations that follow.

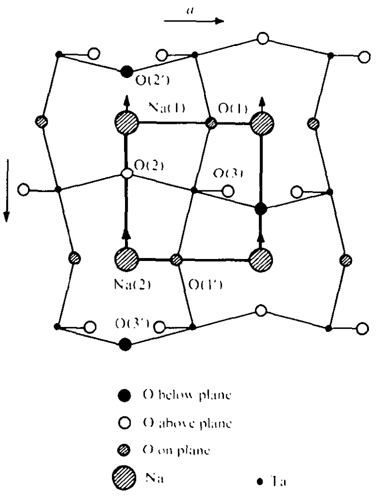

Fig. 2. Diagram of the $NaTaO_3$ $a^0b^+c^-$ structure.

Table 3. *Structural parameters in* $NaTaO_3$ *at* 803 K *with space group Bmmb*

Isotropic temperature factor refinement

		x	y	z	B (Å^2)
Ta	8(*d*)	$\frac{1}{4}$	0	$\frac{1}{4}$	0·78 (3)
Na(1)	4(*c*)	0	$\frac{1}{4}$	−0·021 (5)	4·98 (62)
Na(2)	4(*c*)	0	$\frac{1}{4}$	$\frac{1}{2}$+0·008 (5)	2·44 (71)
O(1)	8(*e*)	$\frac{1}{4}$+0·0185 (12)	0	0	1·89 (11)
O(2)	8(*f*)	0	0·0204 (11)	$\frac{1}{4}$−0·0318 (12)	1·73 (13)
O(3)	8(*g*)	$\frac{1}{4}$+0·0241 (11)	$\frac{1}{4}$	$\frac{1}{4}$−0·0023 (13)	2·40 (11)

$R_{\text{nuclear}} = 11{\cdot}97\%$ $R_{\text{profile}} = 17{\cdot}07\%$ $R_{\text{expected}} = 5{\cdot}95\%$

Anisotropic temperature factor refinement

		B_{eq} (Å^2)
Ta		0·97 (17)
Na(1)	$w_{A1} = -0{\cdot}009$ (4)	3·65 (76)
Na(2)	$w_{A2} = -0{\cdot}025$ (2)	2·65 (72)
O(1)	$u_1 = 0{\cdot}0238$ (13)	2·07 (29)
O(2)	$v_2 = 0{\cdot}0131$ (17), $w_2 = -0{\cdot}0242$ (14)	3·00 (36)
O(3)	$u_3 = 0{\cdot}0256$ (11), $w_3 = 0{\cdot}0016$ (10)	2·28 (32)

$a_p = 7{\cdot}8453$ (5) Å $b_p = 7{\cdot}8541$ (8) Å $c_p = 7{\cdot}8633$ (5) Å

$R_{\text{nuclear}} = 6{\cdot}23\%$ $R_{\text{profile}} = 12{\cdot}93\%$ $R_{\text{expected}} = 5{\cdot}93\%$

Table 4. *Structural parameters in* $NaTaO_3$ *at* 873 K *with space group Bmmb*

Isotropic temperature factor refinement

		B (Å^2)
Ta		0·81 (3)
Na(1)	$w_{A1} = -0{\cdot}007$ (3)	4·59 (42)
Na(2)	$w_{A2} = -0{\cdot}021$ (4)	1·72 (57)
O(1)	$u_1 = +0{\cdot}0149$ (10)	1·70 (22)
O(2)	$v_2 = +0{\cdot}0187$ (11) $w_2 = -0{\cdot}0352$ (9)	1·93 (11)
O(3)	$u_3 = +0{\cdot}0126$ (14) $w_3 = -0{\cdot}0068$ (12)	2·51 (19)

$R_{\text{nuclear}} = 10{\cdot}98\%$ $R_{\text{profile}} = 18{\cdot}18\%$ $R_{\text{expected}} = 4{\cdot}69\%$

Anisotropic temperature factor refinement

		B_{eq} (Å^2)
Ta		0·98 (32)
Na(1)	$w_{A1} = -0{\cdot}020$ (3)	2·17 (73)
Na(2)	$w_{A2} = -0{\cdot}025$ (2)	4·38 (82)
O(1)	$u_1 = 0{\cdot}0172$ (13)	1·73 (39)
O(2)	$v_2 = 0{\cdot}0126$ (18), $w_2 = -0{\cdot}0291$ (13)	3·15 (42)
O(3)	$u_3 = 0{\cdot}0157$ (16), $w_3 = -0{\cdot}0004$ (9)	2·66 (49)

$a_p = 7{\cdot}8560$ (10) Å $b_p = 7{\cdot}8724$ (7) Å $c_p = 7{\cdot}8604$ (9) Å

$R_{\text{nuclear}} = 6{\cdot}60\%$ $R_{\text{profile}} = 14{\cdot}17\%$ $R_{\text{expected}} = 4{\cdot}67\%$

At 803 K the displacements of O(1) along [100] and O(2) along [001] are almost equal, giving the tilt angle $\beta = 5{\cdot}5\ (4)^\circ$. Tilting around [001] displaces O(2) along [010] and O(3) along [100], but in this case there is a distortion of the octahedron, $v_2 \neq u_3$, which gives the average value of the tilt angle $\gamma = 4{\cdot}4\ (15)^\circ$. At 873 K we find $u_1 \neq w_2$, again indicating distorted octahedra, with almost the same average value for $\beta = 5{\cdot}3\ (17)^\circ$ as at 803 K. Instead, the tilting around [001] is clearly smaller at 873 K, $\gamma = 3{\cdot}2\ (7)^\circ$.

5. Structure of $NaTaO_3$ at 893 K

In the neutron powder at 893 K the only superlattice reflections found were those with two indices odd and one even, indicating in-phase tilts of the adjacent octahedra. According to Glazer (1972), this fact, together with the assumption of tetragonal symmetry, suggests the tilt system $a^0b^0c^+$ with the multiple cell $2a_p \times 2b_p \times c_p$ and $a_p = b_p < c_p$. The corresponding space group is $C4/mmb$. In the refinement, the conventional tetragonal axes $\sqrt{2}a_p$, $\sqrt{2}b_p$, c_p (space group symbol $P4/mbm$) were used. The corresponding structural parameters are given in Table 5.

In the tetragonal phase the only distortion from the cubic perovskite form is the rotation of the octahedra through 4·7 (1)° around [001] in the same sense in successive layers. The structure is thus isomorphic with those of $NaNbO_3$ phase T_2 (Glazer & Megaw, 1972), $CsPbCl_3$ phase II (Fujii *et al.*, 1974) and $CsPbBr_3$ phase II (Hirotsu, Harada, Iizumi & Gesi, 1974). If the axes are changed from those in Table 4 to have the b axis as the unique axis, the tilt system is $a^0b^+a^0$.

Table 5. *Structural parameters in* $NaTaO_3$ *at* 893 K *with space group P4/mbm*

Isotropic temperature factor refinement

		x	y	z	B (Å^2)
Ta	2(*a*)	0	0	0	0·84 (3)
Na	2(*c*)	0	$\frac{1}{2}$	$\frac{1}{2}$	3·91 (7)
O(1)	2(*b*)	0	0	$\frac{1}{2}$	2·61 (18)
O(2)	4(*g*)	$\frac{1}{4}$ + 0·0231 (5)	$\frac{1}{4}$ − 0·0231	0	2·70 (8)

$R_{\text{nuclear}} = 13{\cdot}48\%$ $R_{\text{profile}} = 21{\cdot}39\%$ $R_{\text{expected}} = 5{\cdot}92\%$

Anisotropic temperature factor refinement

	B_{eq} (Å^2)			B_{eq} (Å^2)
Ta	0·98 (13)	O(1)		3·21 (23)
Na	3·92 (31)	O(2)	$u_2 = 0{\cdot}0205$ (4)	2·86 (13)

$a_T = b_T = 5{\cdot}5552$ (3) Å $c_T = 3{\cdot}9338$ (4) Å

$R_{\text{nuclear}} = 6{\cdot}45\%$ $R_{\text{profile}} = 14{\cdot}61\%$ $R_{\text{expected}} = 5{\cdot}88\%$

Table 6. *Comparison of the observed* (I_o) *and calculated intensities when the isotropic* [I_c(*iso.*)] *or anisotropic* [I_c(*aniso.*)] *temperature factors are used in the refinements at* 803, 873 *and* 893 K

The reflections are indexed ($h\,k\,l$) with respect to the pseudocubic subcell.

$\Delta(\text{iso.})\% = 100[I_c(\text{iso.}) - I_o]/I_o$

$\Delta(\text{aniso.})\% = 100[I_c(\text{aniso.}) - I_o]/I_o$

	803 K		873 K		893 K	
$h\,k\,l$	Δ(iso.)	Δ(aniso.)	Δ(iso.)	Δ(aniso.)	Δ(iso.)	Δ(aniso.)
1 1 2	−17·0	2·9	−16·6	0·8	−26·2	2·9
1 0 3	59·3	−1·5	38·9	−10·6	55·0	−16·5
2 0 3	45·8	−0·4	34·8	−3·0	44·9	−10·1
1 2 3	21·6	−0·3	17·8	−2·5	22·6	−3·7
3 3 0 1 1 4	−35·7	−4·8	−34·6	−6·3	−45·6	−6·5
1 2 4	−13·8	0·3	−19·1	−1·0	−25·7	−4·3
2 3 3	33·5	−1·3	45·2	3·5	65·1	16·3
2 3 4 2 0 5	17·0	−1·6	24·4	8·3	19·5	−9·0

The inclusion of the anisotropic temperature factors in the refinement lowers the R values considerably, as at 803 K and 873 K. The effect of the anisotropic temperature factors is particularly noticeable in the reflections collected in Table 6. At 803 K the anisotropy explains the difference between the calculated and observed intensities, whereas at higher temperatures the agreement is less good, possibly indicating anharmonic vibrations.

6. Discussion

The first part deals with crystallographic aspects, comparing bond lengths, atomic environments *etc.*, found in $NaTaO_3$ with those in $NaNbO_3$ and $SrZrO_3$. In the second part we shall deal more with the nature of the phase transitions in these materials and analyse the structures in terms of condensed normal modes of the cubic, high-temperature phase.

6*A*. *Crystallographic aspects*

One might expect from chemical considerations that $NaTaO_3$ and $NaNbO_3$ would undergo similar structural changes as a function of temperature. Indeed, this is so at high temperatures: the two highest-temperature transitions occur at 903 K and 853 K in $NaTaO_3$ and at 913 K and 848 K in $NaNbO_3$. The three phases separated by these transitions have octahedral tilt systems $a^0a^0a^0$, $a^0b^+a^0$ and $a^0b^+c^-$.*

However, at 793 K $NaNbO_3$ changes its structure to tilt system $a^+b^+c^-$, while $NaTaO_3$ changes at 753 K to $a^-b^+a^-$. It is interesting to note that in both these latter phases the symmetry at the B site is $\bar{1}$, but the point symmetry at the Na site in $a^+b^+c^-$ is mm while in $a^-b^+a^-$ it is only m. In $SrZrO_3$ the sequence of the tilt systems with decreasing temperature is $a^0a^0a^0$, $a^0a^0c^-$, $a^0b^+c^-$, $a^-b^+a^-$. It differs, thus, from $NaTaO_3$ only in the tetragonal phase.

The room-temperature structure of $NaTaO_3$ is in almost all aspects simpler than the corresponding phase P of $NaNbO_3$ (Sakowski-Cowley, Lukaszewicz & Megaw, 1969). For example, in phase P, Nb atoms are displaced antiparallel almost perpendicular to the [010] direction – this off-centring giving rise to the antiferroelectric properties of $NaNbO_3$; the Nb–O distances vary between 1·857 and 2·110 Å, the mean value being 1·986 Å. In $NaTaO_3$, on the other hand, the heavy Ta atoms are at the centres of the O octahedra, with a mean Ta–O distance of 1·978 Å and extreme values of 1·973 and 1·982 Å, giving a 'strain'

---

* One cannot be certain whether in going from $a^0b^+a^0$ to the next lower phase the tilt system is $a^0b^+c^-$ or $a^0b^-c^+$ without carrying out a single-crystal study.

of 0·5%. In the isostructural room-temperature phase of $SrZrO_3$ (Ahtee *et al.*, 1976) the corresponding mean Zr—O distance is 2·091 Å, with extreme values of 2·084 and 2·095 Å, giving the same amount of strain.

Phase *P* of $NaNbO_3$ has tilts similar to those in $NaTaO_3$ for a double sheet of octahedra parallel to [010] possessing a mirror plane, but this double sheet is then operated on by a diad screw axis to give a unit cell four octahedra high. This rather complicated system gives rise to two different Na surroundings: Na(1), lying on the diad axis, is almost undisplaced, while Na(2), on the mirror plane, has a large displacement, 0·18 Å, in the same direction as Nb. When the Na environments are examined in order to find a set of nearly equal Na—O bonds it is found that Na(1) in $NaNbO_3$ is surrounded by a triangle of O atoms whereas Na(2) is surrounded by a tetrahedron. As pointed out by Megaw, the rather unusual Na(1) environment is the less-stable one, and therefore one expects to find configurations more like that of Na(2). Indeed, the Na environment in $NaTaO_3$ is similar to that of Na(2) in $NaNbO_3$; in $NaNbO_3$ there are three O atoms at 2·52 and one at 2·39 Å from Na; in $NaTaO_3$ there are three O atoms at 2·43 and one at 2·67 Å. In $SrZrO_3$, the Sr environment is again similar to that of Na(2); now there is one O at 2·50, two at 2·57 and one at 2·69 Å, forming the tetrahedral environment.

$NaTaO_3$ at 803 and 873 K, $NaNbO_3$ (phase T_1) (Ahtee, Glazer & Megaw, 1972) and $SrZrO_3$ at 1033 K (Ahtee, Glazer & Hewat, 1978) are all isostructural; they have the same space group *Bmmb* and the tilt system $a^0b^+c^-$. To obtain a better comparison we redetermined the structure of $NaNbO_3$ (T_1) by the neutron powder profile-refinement technique. The results are given in Table 7. For a closer comparison of the three isostructural phases the interatomic distances are collected in Table 8 and the tilt angles and *A*-cation displacements are compared in Table 9. From the latter, the reversal of the magnitudes of the tilt angles and *A*-cation displacements in $SrZrO_3$ compared with those in $NaTaO_3$ and $NaNbO_3$ can be seen.

Table 7. *Structural parameters in* $NaNbO_3$ (*phase* T_1) *at* 813 K *with space group Bmmb*

Isotropic temperature factor refinement

		B (Å²)
Nb		1·02 (2)
Na(1)	w_{A1} = 0·017 (5)	3·79 (52)
Na(2)	w_{A2} = −0·016 (4)	4·08 (47)
O(1)	u_1 = 0·0257 (12)	1·93 (11)
O(2)	v_2 = 0·0228 (8) w_2 = −0·0298 (12)	2·16 (10)
O(3)	u_2 = 0·0194 (9) w_3 = −0·0020 (13)	2·38 (9)

$R_{nuclear}$ = 10·36% $R_{profile}$ = 16·15% $R_{expected}$ = 5·07%

Anisotropic temperature factor refinement

		B_{eq} (Å²)
Nb		1·18 (16)
Na(1)	w_{A1} = −0·007 (3)	2·94 (50)
Na(2)	w_{A2} = −0·011 (4)	5·48 (77)
O(1)	u_1 = 0·0285 (10)	2·46 (24)
O(2)	v_2 = 0·0191 (10), w_2 = −0·0237 (10)	2·43 (22)
O(3)	u_3 = 0·0177 (9), w_3 = −0·0022 (11)	2·80 (23)

a_p = 7·8592 (3) Å b_p = 7·8662 (3) Å c_p = 7·8773 (2) Å

$R_{nuclear}$ = 4·45% $R_{profile}$ = 10·59% $R_{expected}$ = 5·05%

Table 8. *Comparison of the interatomic distances in* $NaTaO_3$ (803 K), $NaNbO_3$ (813 K) *and* $SrZrO_3$ (1033 K) *all having the same tilt system* $a^0b^+c^-$

Numbers in square brackets indicate the number of equivalent bonds.

	$NaTaO_3$	$NaNbO_3$	$SrZrO_3$
a_p	7·8453 (5) Å	7·8592 (3) Å	8·2532 (3) Å
b_p	7·8541 (8)	7·8662 (3)	8·2662 (5)
c_p	7·8633 (5)	7·8773 (2)	8·2709 (4)
B—O(1)	1·975 (1)	1·982 (1)	2·070 (1)
O(2)	1·973 (2)	1·979 (2)	2·086 (3)
O(3)	1·974 (1)	1·972 (1)	2·093 (2)
Mean	1·974 (1)	1·978 (1)	2·083 (2)
A(1)—O(1)	2·911 (9) [4]	2·943 (6) [4]	2·989 (11) [4]
O(2)	2·621 (40) [2]	2·584 (28) [2]	2·708 (28) [2]
O(2′)	2·679 (38) [2]	2·732 (26) [2]	3·005 (25) [2]
O(3)	2·979 (34) [2]	2·908 (27) [2]	3·254 (26) [2]
O(3′)	2·577 (35) [2]	2·658 (28) [2]	2·594 (28) [2]
Mean	2·780 (27)	2·795 (20)	2·923 (22)
A(2)—O(1)	2·654 (8) [4]	2·628 (6) [4]	2·855 (10) [4]
O(2)	2·702 (29) [2]	2·753 (35) [2]	2·793 (28) [2]
O(2′)	3·131 (29) [2]	3·084 (34) [2]	3·228 (27) [2]
O(3)	2·786 (22) [2]	2·835 (32) [2]	3·113 (26) [2]
O(3′)	2·798 (24) [2]	2·737 (34) [2]	2·757 (28) [2]
Mean	2·788 (20)	2·778 (25)	2·934 (22)

Table 9. *Tilt angles* (°) *and A-cation displacements* (Å) *in* $NaTaO_3$ *at* 803 K *and* 873 K, $NaNbO_3$ *at* 813 K *and* $SrZrO_3$ *at* 1033 K

	$NaTaO_3$		$NaNbO_3$	$SrZrO_3$
	803 K	873 K	813 K	1033 K
A(1)	0·07 (3)	0·16 (3)	0·06 (3)	0·09 (2)
A(2)	0·20 (2)	0·20 (2)	0·09 (3)	0·03 (2)
β	5·5 (4)	5·3 (17)	6·0 (8)	3·1 (6)
γ	4·4 (15)	3·2 (7)	4·2 (4)	8·5 (3)

The Ta—O distances are now almost equal to the mean value of 1·974 Å, whereas in $NaNbO_3$ the bonds Nb—O(3) = 1·972 Å are clearly shorter than the mean value of 1·978 Å. In $SrZrO_3$, the smallest distance is Zr—O(1) = 2·065 Å compared to the mean value of 2·079 Å. In all the three cases the *A*(1) cation is tetrahedrally bound between O(2) and O(3′), as is Sr(2) in $SrZrO_3$, while the four O(1) atoms forming an approximate square are the nearest neighbours of Na(2). The notation in Fig. 2 is used for all three structures.

In $NaTaO_3$, the O octahedra are very regular so that we can consider the effects of the O displacements on the Na cations in terms of the tilts. The γ tilt around [001] through O(3′) and the β tilt around [010] through O(1′) push Na(2) along [001]. Again tilts β and γ *via* O(2) push Na(1) along [001], but they are opposed by O(3′). In the next layer along [010], the displacements of Na are exactly opposite. In $NaNbO_3$, the space between the Na octahedra is greater and also the O(3) atoms are more closely bound to the *B* cation than in $NaTaO_3$ so that the Na displacements are understandably smaller. In $SrZrO_3$, the O(1) atoms are even more closely bound to Zr, which may explain why the β tilt is smaller than in $NaTaO_3$ or $NaNbO_3$.

As the Na atom is lighter than Sr it seems likely that even a small O displacement will displace it significantly, *e.g.* the γ tilt through O(3′) displaces Na(2) but only slightly affects Sr(2). Thus, one can understand why the antiphase γ tilt has to disappear together with Na displacements in going to the tetragonal phases of $NaTaO_3$ and $NaNbO_3$ (Glazer & Megaw, 1972). In $SrZrO_3$, instead, the antiphase tilting of the successive octahedra, an energetically and crystallographically more stable arrangement, is favoured in the tetragonal phase. In the tilt system $a^0b^+a^0$ the four next-nearest O atoms form a square around the *A* cation, whereas in the tilt system $a^0a^0c^-$ they form a tetrahedron.

From their neutron powder profile refinement of the high-temperature structures of $SrZrO_3$, Ahtee, Glazer & Hewat (1978) concluded that the unusually anisotropic thermal ellipsoids provide evidence for the existence of low-frequency vibrational modes in this material. The behaviour of the anisotropic temperature factors in the corresponding phases in $NaTaO_3$ is very similar. Both in the tetragonal and in the next lower phase the directions of the smallest O atom motions are along Ta—O bonds. The anisotropic temperature factors of the O atoms are thus consistent with the rigid-body vibration of the O octahedron. By dividing the largest vibrational amplitudes into two components it is possible to interpret their motion due to the condensation of soft modes to give tilts in the successive phases.

6*B*. *Soft modes in the cubic phase and the crystal structure of the low-temperature phase*

$NaTaO_3$ is one of many perovskites that exhibit a number of phases in which the octahedra are rotated or tilted about pseudocubic ⟨100⟩ directions. It seems well established that transitions of this type are caused by condensation of normal modes of vibration, and that the static displacements found in each low-temperature phase may be described as condensed modes of the cubic phase. This latter observation seems to apply even though the low-temperature form may not transform directly into the cubic phase itself, but first into another modification of the cubic structure.

A knowledge of the space group of a low-temperature phase allows one to determine which normal modes of the cubic phase are allowed to be present in the structure, in other words, which irreducible representations are compatible with the group G_o of the cubic phase and the sub-group G_s of the distorted structure. Ignoring acoustic modes at the zone centre, the number of irreducible representations equals the number of atomic positional parameters needed to specify the structure.

Structure determinations give the actual atomic displacements and from these the amplitudes of the condensed modes in each structure can be calculated. Following Cochran & Zia (1968) it is perhaps more appropriate to calculate the quantity W defined as

$$W = \frac{v}{v'} \sum_{lk} m_k\, u^2(lk,\mathbf{q}R)$$

where v and v' are the volumes of the cubic and low-temperature forms, m_k the mass of atom k, and $\mathbf{u}(lk,\mathbf{q}R)$ the displacement of atom k by mode $(\mathbf{q}R)$ acting on its own.

Unfortunately, in only a few cases where more than one octahedral rotation is present in the structure has it been possible to allow the refinement of the structure to

Table 10. *Condensed modes and their strengths, W*

	Mode		$NaTaO_3$ (RT) *Pcmn* $a^-b^+a^-$	$SrZrO_3$ (RT) *Pcmn* $a^-b^+a^-$	$NaTaO_3$ (803 K) *Bmmb* $a^0b^+c^-$	$NaTaO_3$ (873 K) *Bmmb* $a^0b^+c^-$	$SrZrO_3$ (1033 K) *Bmmb* $a^0b^+c^-$	$NaNbO_3$ (813 K) *Bmmb* $a^0b^+c^-$	$NaTaO_3$ (893 K) *P4/mbm* $a^0b^+a^0$	$SrZrO_3$ (1173 K) *I4/mcm* $a^0a^0c^-$
A	$0\frac{1}{2}0, M'_5$		0·175	2·010	0·40	0·719	0·295	0·115	0	0
A	$\frac{1}{2}\frac{1}{2}\frac{1}{2}, R_{15}$		0·015	0·027	0·091	0·009	0·330	0·006	0	0
B	None									
O	$\frac{1}{2}0\frac{1}{2}, M_3$	OR	2·316	2·581	1·137	1·064	0·344	1·348	0·830	0
O	$\frac{1}{2}0\frac{1}{2}, M_1$	OD	0·0001	0·0008	0·0001	0·071	0·003	0·011	0	0
O	$\frac{1}{2}\frac{1}{2}\frac{1}{2}, R_{25}$	OR	3·534	5·49	0·740	0·399	3·060	0·671	0	1·693
O	$\frac{1}{2}\frac{1}{2}\frac{1}{2}, R_{15}$	OD	0·002	0·002	0·077	0·005	0·014	0·001	0	0
O	$0\frac{1}{2}0, M'_5$	OD	0·041	0·175	0·003	0·0002	0·038	0·005	0	0

proceed without restraints placed upon the parameters, such as restricting the octahedra to remain regular. Included in the exceptions are the low-temperature forms of $NaTaO_3$ and $NaNbO_3$ (T_1) reported here, and those of $SrZrO_3$. In Table 10 these structures are analysed in terms of the full set of normal modes of the cubic phase. The notation for the irreducible representations follows that of Cowley (1964) with the exception that the zone-corner modes will be labelled R_{15}, R_{25} rather than Γ_{15}, Γ_{25}. OR stands for octahedral rotation or tilt, and OD indicates a mode that distorts the octahedra.

In the phases $a^-b^+c^-$ and $a^0b^+c^-$ the same seven modes with non-zero wavevectors are required to specify the atomic displacements, while only one is needed for both $a^0b^+a^0$ and $a^0a^0c^-$. Modes $[(\frac{1}{2}\frac{1}{2}\frac{1}{2}), R_{15}]$ and $[(\frac{1}{2}\frac{1}{2}\frac{1}{2}), R_{25}]$ are triply degenerate in the cubic phase, and in $a^-b^+a^-$ two components have condensed out with equal magnitude (these could be labelled the x and z components) while in $a^0b^+c^-$ only the z component is present. The modes described by $[(0\frac{1}{2}0), M_5']$ are doubly degenerate in the cubic phase: in $a^-b^+a^-$ both components are present in equal amounts while in $a^0b^+c^-$ only the z component is non-zero. Both $[(\frac{1}{2}0\frac{1}{2}), M_1]$ and $[(\frac{1}{2}0\frac{1}{2}), M_3]$ are singlets.

One encouraging aspect of the result is that only two or three modes appear with significant weight in the different materials. The most important are those that correspond to rotating rigid octahedra in the cubic phase. Clearly, all modes which involve departure from regularity for the octahedra are weak; the strongest is the mode $[(0\frac{1}{2}0), M_5']$ involving only one of the O atoms: the A atoms can also be displaced in a similar fashion. The presence of this mode in these structures was proposed earlier (Darlington, 1976).

One might anticipate that the modes $[(\frac{1}{2}0\frac{1}{2}), M_3]$, $[(\frac{1}{2}\frac{1}{2}\frac{1}{2}), R_{25}]$ and $[(0\frac{1}{2}0), M_5']$ should be of low frequency in the cubic phase. The most detailed experimental evidence has been obtained by Stirling (1972) for $SrTiO_3$. The first two, the octahedral rotational modes, do have anomalously low frequencies at room temperature, as they do in many cubic perovskites. Experimentally, the modes with the next-lowest frequency in $SrTiO_3$ are $[(\frac{1}{2}\frac{1}{2}0), M_2']$, $[(\frac{1}{2}\frac{1}{2}0), M_3']$ and $[(\frac{1}{2}\frac{1}{2}0), M_5']$, none of which are found in any of the structures in Table 10. In fact, these modes are incompatible with the sub-group G_s of each of the distorted structures.

It is interesting to restate the point (Glazer, 1976) that the overall symmetry of a non-ferroelectric low-temperature perovskite phase appears to be determined by the octahedral tilt system. Writing atomic displacements in the cubic crystal as

$$u(lk) = (Nm_k)^{-1/2} \sum_{\mathbf{q}j} Q(\mathbf{q}j)\, e(k,\mathbf{q}j) \times \exp\{i\mathbf{q}.[r(l) + r(k)]\},$$

the difference in free energy between the distorted and cubic phases is given by

$$\Delta F = \frac{1}{2} \sum_{\mathbf{q}j} \omega^2(\mathbf{q}j)\langle Q(\mathbf{q}j)\rangle^2 + \frac{1}{n!} \sum_{n>2} \sum_{\mathbf{q}_1j_1\ldots\mathbf{q}_nj_n} V^{(n)} \times (\mathbf{q}_1j_1\ldots\mathbf{q}_nj_n)\langle Q(\mathbf{q}_1j_1)\ldots Q(\mathbf{q}_nj_n)\rangle \qquad (1)$$

where $\langle Q\rangle$ is the static value of a normal coordinate. The coefficients $V^{(n)}$ are zero unless the wavevectors involved satisfy the condition

$$\sum \mathbf{q}_i = \mathbf{H},$$

where $\mathbf{H}$ is a vector of the reciprocal lattice.

The fact that the symmetry appears to be determined by the octahedral tilt system alone in $NaTaO_3$ and $SrZrO_3$ suggests that the only soft modes in their cubic structures are octahedral tilting modes. Non-zero values of $\langle Q\rangle$ for other modes occur because the anharmonic coefficients $V^{(n)}$ coupling these modes to octahedral rotational modes are large, making the second term in (1) outweigh the positive contribution from the first term for that mode.

In $NaNbO_3$, where the Nb atom is displaced in an antiparallel array at room temperature, and in a parallel fashion at low-temperatures (Darlington & Megaw, 1973), it seems extremely probable that in addition to soft octahedral rotational modes, one of the transverse optic branches has low frequency over a large range of q values stretching from the zone centre out towards the X point of the cubic Brillouin zone.

One of us (MA) gratefully acknowledges a grant from the Natural Science Council of the Finnish Academy. She also wishes to thank Dr A. W. Hewat for assistance at the Institut Laue–Langevin, Grenoble. Both of us would like to thank Dr H. D. Megaw for her continuing interest and helpful advice.

References

Ahtee, A., Ahtee, M., Glazer, A. M. & Hewat, A. W. (1976). *Acta Cryst.* B**32**, 3243–3246.

Ahtee, M., Glazer, A. M. & Hewat, A. W. (1978). *Acta Cryst.* B**34**, 752–758.

Ahtee, M., Glazer, A. M. & Megaw, H. D. (1972). *Philos. Mag.* **26**, 995–1014.

Ahtee, M. & Unonius, L. (1977). *Acta Cryst.* A**33**, 150–154.

Bacon, G. E. (1972). *Acta Cryst.* A**28**, 357–358.

Cochran, W. & Zia, A. (1968). *Phys. Status Solidi*, **25**, 273–283.

Cowley, R. A. (1964). *Phys. Rev. Sect. A*, **134**, 981–997.

Cross, L. E. (1956). *Philos. Mag.* **1**, 76–92.

Darlington, C. N. W. (1976). *Phys. Status Solidi B*, **76**, 231–239.

Darlington, C. N. W. & Megaw, H. D. (1973). *Acta Cryst.* B**29**, 2171–2185.

Fujii, Y., Hoshino, S., Yamada, Y. & Shirane, G. (1974). *Phys. Rev. B*, **9**, 4549–4559.

GLAZER, A. M. (1972). *Acta Cryst.* B**28**, 3384–3392.
GLAZER, A. M. (1976). *Acta Cryst.* A**31**, 756–762.
GLAZER, A. M. & MEGAW, H. D. (1972). *Philos. Mag.* **25**, 1119–1135.
HEWAT, A. W. (1973). *J. Phys. C*, **6**, 2559–2572.
HEWAT, A. W. & BAILEY, I. (1976). *Nucl. Instrum. Methods*, **137**, 463–471.
HIROTSU, S., HARADA, J., IIZUMI, M. & GESI, K. (1974). *J. Phys. Soc. Jpn*, **37**, 1393–1398.
ISMAILZADE, I. G. (1963). *Sov. Phys. Crystallogr.* **7**, 584–587.
IWASAKI, H. & IKEDA, T. (1963). *J. Phys. Soc. Jpn*, **18**, 157–163.
KAY, H. F. & MILES, J. L. (1957). *Acta Cryst.* **10**, 213–218.
RIETVELD, H. M. (1969). *J. Appl. Cryst.* **2**, 65–71.
SAKOWSKI-COWLEY, A. C., LUKASZEWICZ, K. & MEGAW, H. D. (1969). *Acta Cryst.* B**25**, 851–865.
STIRLING, W. G. (1972). *J. Phys. C*, **5**, 2711–2730.
WILLIS, B. T. M. & PRYOR, A. W. (1975). *Thermal Vibrations in Crystallography*, pp. 101–102. Cambridge Univ. Press.

Acta Cryst. (1980). B**36**, 1014–1017

Bis(trichlorophosphine)iminium Hexachlorophosphate*

BY R. FAGGIANI, R. J. GILLESPIE, J. F. SAWYER AND J. D. TYRER

Department of Chemistry, McMaster University, Hamilton, Ontario, Canada L8S 4M1

(*Received* 17 *July* 1979; *accepted* 19 *November* 1979)

Abstract

$[Cl_3PNPCl_3][PCl_6]$ is monoclinic, $P2_1/c$, with a = 11·692 (5), b = 20·898 (9), c = 15·872 (6) Å, β = 119·00 (3)°, Z = 8 (two independent molecules), D_c = 2·08 Mg m^{-3}. The structure was solved by direct methods and refined by least squares to a final R_1 = 0·052 for 1575 observed reflections. The cations in the structure have *cisoid* configurations with P—N distances of 1·51–1·56 Å and PNP angles of 135·7 (8) and 139·0 (8)°. The P—Cl distances (uncorrected for thermal effects) are in the range 2·101 (7)–2·146 (6) Å in the anion and 1·924 (7)–1·962 (7) Å in the cation.

Introduction

As part of a continuing study of the reactions of sulphur–nitrogen compounds with Lewis acids, the reaction of S_7NH with $SbCl_5$ has recently been shown to produce the dithionitronium cation NS_2^+ (Faggiani, Gillespie, Lock & Tyrer, 1978), whilst reactions of S_7NH (and $S_4N_4H_4$) with the oxidant PF_5 have so far been observed to produce only $NH_4^+PF_6^-$ and sulphur. However, the analogous reaction of S_7NH with PCl_5 in a 1:2 molar ratio in CH_2Cl_2 gave a complex mixture of solid products, one of which has been identified in this study as the title compound. A small approximately spherical crystal of radius 0·1 mm was selected from the reaction products and sealed in a Lindemann capillary. Accurate unit-cell dimensions were obtained by least-squares refinement with 15 high-angle reflections measured on a Syntex $P2_1$ diffractometer using Mo $K\alpha$ radiation (λ = 0·71069 Å). Data were collected to a maximum 2θ of 35° using θ–2θ scans over a 2θ scan range ($K\alpha_1$ − 1·0°) to ($K\alpha_2$ + 1·0°) with the variable scan rate of 8·0–29·3° min^{-1} depending on the intensity of a preliminary count. The crystal was recentred several times during the data collection. 2000 data were collected and corrections for Lorentz and polarization effects were applied. No absorption corrections were considered necessary (μ = 2·2 mm^{-1} and μR = 0·22). No experimental density was measured due to the moisture sensitivity of the crystal and because it was isolated from a mixture of products.

Although the composition of the crystal was initially unknown, a suitable number of S and N atoms in the unit cell was assumed for the calculation of normalized structure factors and the structure solution was attempted using the direct-method routines of the program *SHELX* (Sheldrick, 1976). Two octahedral PCl_6^- groups found in one of the several E maps calculated were sufficient to phase a subsequent Fourier map which revealed the two $[Cl_6P_2N]^+$ cations. Atomic assignments in these cations were made on the basis of other data. The single-crystal Raman spectrum of the cation is comparable to that previously published (Baumgaertner, Sawodny & Goubeau, 1965) although more bands were observed (Table 1), presumably due to solid-state crystal effects. The ^{31}P NMR spectrum of

---

* Alternative name: Trichloro[(trichlorophosphoranylidene)-iminio]phosphorus(V) hexachlorophosphate.

0567-7408/80/051014-04$01.00